Semiclassical behavior at a quantum avoided crossing

Marc Joyeux
Laboratoire de Spectrométrie Physique (CNRS UA08), Université Joseph Fourier-Grenoble I, BP 87, 38402 St Martin d'Hères Cedex, France

(Received 9 August 1994; accepted 7 November 1994)

For a polynomial potential with resonant fundamental frequencies (1:2 and 1:3 resonances), quantum avoided crossings can occur when quantum eigenvalues are plotted versus a parameter in the Hamiltonian. In the present paper, primitive (EBK) semiclassical behavior at the quantum avoided crossing is reinvestigated, using the exact analytical calculation of the action integrals, which was devised recently [Chem. Phys. **185**, 263 (1994)] for an approximate resonance Hamiltonian that can be deduced from the exact polynomial Hamiltonian by low order perturbation theory. The previously reported behavior, that is semiclassical levels passing through the intersection instead of avoiding each other, is shown to happen if there exist two superimposed branches in the plot of the second action integral $\mathscr{I}_2$ as a function of the energy. These results are interpreted in terms of semiclassical diabatic basis and of quantum dynamical tunneling. In contrast, if the semiclassical system enters the (anti)crossing region with semiclassical quantum numbers $\mathscr{I}_2$ which do not lie on superimposed branches of the plot, it is shown that at least one, and possibly two, level(s) must cross the separatrix, that is pass from the inside to the outside of the resonance region (or conversely) in order to adapt to the quantum avoided crossing. This causes (i) corresponding semiclassical quantum number $\mathscr{I}_2$ to change (ii) the close correspondence between quantum and semiclassical mechanics to break down.

I. INTRODUCTION

In the context of the quantum study of coupled anharmonic vibrations described by a polynomial Hamiltonian, avoided crossings (or ''anticrossings'') occur in the plot of energy levels versus the value of one of the coupling parameters in the polynomial expansion. Two levels are said to anticross if a naive linear extrapolation of their energies observed outside the anticrossing region predicts that they should cross, whereas they actually approach each other more or less closely without intersecting. Avoided crossings produce local changes in the spectrum, which becomes more rigid since levels repel each other, and dramatic changes in the wave functions of participating levels.

The interesting question of the classical and semiclassical behavior of two anharmonically coupled oscillators at an avoided crossing has been addressed some years ago[1–3] for a fourth order polynomial Hamiltonian in the regular (nonchaotic) region. From the semiclassical point of view, it was found that semiclassical eigenvalue plots passed through the intersection instead of avoiding each other,[1] which in turn lead to the conclusion that the splitting is due to a classically forbidden process. A ''uniform'' semiclassical quantization procedure was therefore proposed[2,3] to override this discrepancy and was claimed to give anticrossing semiclassical levels.

This paper is devoted to the reinvestigation of the ''primitive'' (EBK) semiclassical behavior at a quantum avoided crossing, the study of which appears not to be complete in Refs. 1–3, using the exact analytical calculation of the action integrals of an approximate resonance Hamiltonian, which was devised recently.[4] The outline of the paper is as follows. Section II deals with the reduction of the full polynomial Hamiltonian to the approximate resonance Hamiltonian and with the calculation of quantum and semiclassical levels. Restrictions due to the use of the approximate resonance Hamiltonian are pointed out. Semiclassical behavior at the quantum avoided crossing is then discussed in Sec. III. Finally, the Appendix deals with the calculation of the energy of the singular points in the plot of the second action integral, which play a central role in Sec. III.

II. QUANTUM AND SEMICLASSICAL ENERGY LEVELS

A. Reduction to the resonance Hamiltonian

The avoided crossing problem studied in Refs. 1 and 2 deals with the polynomial Hamiltonian

$$H(p_x,p_y,x,y)=\tfrac{1}{2}\,(p_x^2+p_y^2+\omega_x^{02}x^2+\omega_y^{02}y^2) -a(x^3+y^3)+\lambda x^2y^2-bxy^n, \qquad (2.1)$$

where $\omega_x^0\approx n\omega_y^0$. In Refs. 1 and 2, the case $n=3$ was actually studied, but extension to the 1:2 resonance is straightforward. Semiclassical quantization of the Hamiltonian in Eq. (2.1) is quite cumbersome and requires calculation of areas in well-chosen Poincaré surfaces of section. In order to avoid this lengthy procedure, a simpler Hamiltonian (simpler in the sense that its semiclassical quantization is known analytically) can be derived, which exhibits the main features of the Hamiltonian in Eq. (2.1)—and particularly avoided crossings. This is achieved by application of fourth order Birkhoff–Gustavson perturbation theory (BGPT)[2,5–7] followed by a canonical transformation to action anglelike coordinates (I_i,φ_i)

$$x=\sqrt{\frac{2I_1}{\omega_x^0}}\cos\varphi_1, \quad p_x=-\sqrt{2\omega_x^0 I_1}\sin\varphi_1 \qquad (2.2)$$

 0021-9606/95/102(7)/2816/9/$6.00

and similar relations for y, p_y, φ_2, and I_2. BGPT consists of successive canonical transformations of increasing orders, which retain at a given order only those terms, which either do not depend on φ_1 and φ_2 or depend on the slow-varying angle $\varphi_1-n\varphi_2$. One obtains

$$H(I_1,I_2,\varphi_1,\varphi_2)=\omega_1 I_1+\omega_2 I_2+x_{11}I_1^2+x_{22}I_2^2+x_{12}I_1I_2 + 2k_{mn}I_1^{1/2}I_2^{n/2}\cos(\varphi_1-n\varphi_2) \quad (2.3)$$

with

$$\omega_1=\omega_x^0,\quad \omega_2=\omega_y^0,\quad x_{11}=-\frac{15a^2}{4\omega_x^{04}},\quad k_{mn}=-\frac{b}{\sqrt{2^{n+1}\omega_x^0\omega_y^{0n}}}. \quad (2.4)$$

and, if $n=2$

$$x_{12}=\frac{\lambda}{\omega_x^0\omega_y^0}-\frac{b^2}{2\omega_x^0\omega_y^{02}(\omega_x^0+2\omega_y^0)}-\frac{3ab}{\omega_x^{03}\omega_y^0},$$

$$x_{22}=-\frac{15a^2}{4\omega_y^{04}}-\frac{b^2(5\omega_x^0+8\omega_y^0)}{8\omega_x^{02}\omega_y^{02}(\omega_x^0+2\omega_y^0)},$$

or, if $n=3$

$$x_{12}=\frac{\lambda}{\omega_x^0\omega_y^0},\quad x_{22}=-\frac{15a^2}{4\omega_y^{04}}.$$

It is worth noting that the Hamiltonian in Eq. (2.3) is that one used by spectroscopists to fit vibrational spectra of molecules with two modes in near 1:n resonance.[8–10]

B. Quantum levels

The full and approximate Hamiltonians in Eqs. (2.1) and (2.3) are rewritten in terms of the dimensionless coordinates

$$p_1=\frac{p_x}{\sqrt{\omega_x^0}},\quad q_1=\sqrt{\omega_x^0}x,\quad p_2=\frac{p_y}{\sqrt{\omega_y^0}},\quad q_2=\sqrt{\omega_y^0}y \quad (2.5)$$

and of the raising and lowering operators

$$a_i^+=\frac{1}{\sqrt{2}}(q_i-jp_i),\quad a_i=\frac{1}{\sqrt{2}}(q_i+jp_i). \quad (2.6)$$

The calculation for the full polynomial Hamiltonian in Eq. (2.1) is straightforward. For the approximate Hamiltonian in Eq. (2.3), one obtains

$$H=\omega_1 d_1+\omega_2 d_2+x_{11}d_1^2+x_{22}d_2^2+x_{12}d_1d_2 + k_{mn}(a_1^+a_2^n+a_1a_2^{+n}), \quad (2.7)$$

where

$$d_i=\tfrac{1}{2}(p_i^2+q_i^2) \quad (2.8)$$

is a diagonal operator. The quantum energy levels for the full and approximate Hamiltonians are then obtained by diagonalization of the Hamiltonian matrix in the $|v_1,v_2\rangle=|v_1\rangle\otimes|v_2\rangle$ basis set of the harmonic oscillator, using the well-known matrix elements for p_i, q_i, d_i, a_i, and a_i^+.

For the approximate resonance Hamiltonian in Eqs. (2.3) and (2.7), there is a single off-diagonal coupling term: $|v_1,v_2\rangle$ is coupled only to $|v_1\pm1,v_2\mp n\rangle$. Stated in other words, the approximate Hamiltonian only couples basis levels which share the same "polyad" number $i=nv_1+v_2$, and levels belonging to the same polyad are obtained by diagonalization of a tridiagonal finite-size matrix with size $1+E(i/n)$. The polyad number i remains a good quantum number, whereas neither v_1 nor v_2 do.

For the full polynomial Hamiltonian, the number of off-diagonal elements is much higher than for the approximate Hamiltonian. There are 10 off-diagonal terms for $n=2$ and 12 terms for $n=3$. These terms couple basis levels belonging to the same polyad, but also levels with different polyad numbers. Therefore, the polyad number is no longer a good quantum number for this Hamiltonian. A further consequence is that calculation of energy levels theoretically requires diagonalization of an infinite-size matrix. For numerical calculation purposes, it was, however, found that increasing v_1 from 0 to 6 (respectively, from 0 to 5) and v_2 from 0 to 12 (respectively, from 0 to 15) for the 1:2 resonance (respectively, the 1:3 resonance) leads to absolute errors lower than 10^{-5} for the low-lying energy levels reported in this paper. The corresponding sizes of the Hamiltonian matrices are only 91×91 for the 1:2 resonance and 96×96 for the 1:3 resonance.

In Fig. 1, the exact and approximate (BGPT) quantum energy levels are drawn for increasing values of λ for the three examples that are going to be discussed in this paper. It is seen that Eq. (2.3) is a particularly close approximation of Eq. (2.1) for the last two examples, which correspond to low values of the anharmonicities (parameter a) and of the resonance coupling (parameter b), and for which the avoided crossing occurs at low values of the parameter λ. The exact energy values of the levels do not agree that well for the first example, but the position and the width of the avoided crossing are nevertheless correctly reproduced, which is the only really important point.

The fact that the approximate Hamiltonian only couples levels belonging to the same polyad, whereas the full Hamiltonian contains much more coupling terms, restricts the validity of this study to almost exact 1:2 or 1:3 resonances, that is to fundamental frequencies such that ω_x^0 and $n\omega_y^0$ are almost equal, and to levels lying at relatively low energy, in the region where different polyads do not overlap. Indeed, these two conditions are needed to ensure that all the avoided crossings observed for the full Hamiltonian occur for levels belonging to the same polyad of the approximate Hamiltonian and therefore also anticross for this Hamiltonian.

C. Semiclassical levels

Exact analytical semiclassical quantization of the approximate Hamiltonian in Eq. (2.3) was studied at length in a recent paper.[4] For the sake of being complete, the final result is reproduced below. The two action integrals $\mathscr{I}_1$ and $\mathscr{I}_2$ of the approximate Hamiltonian in Eq. (2.3) are

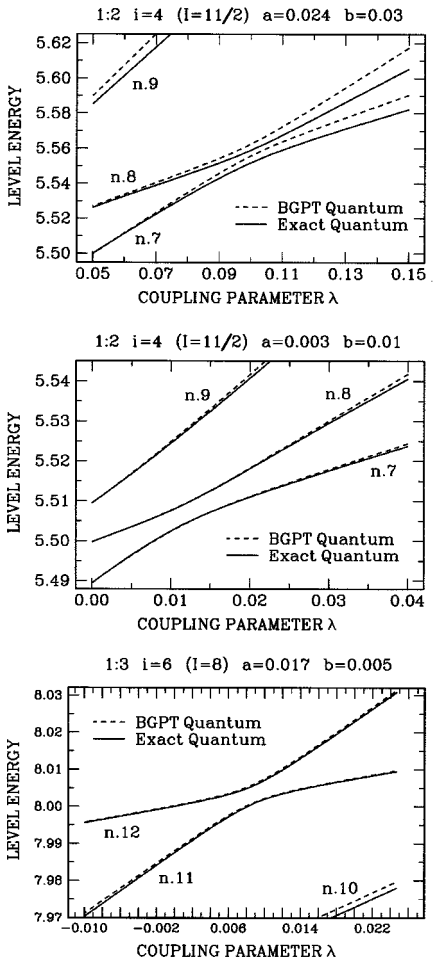

FIG. 1. Plot of exact [Eq. (2.1)] and approximate [Eq. (2.7)] quantum levels as a function of the parameter λ for three different sets of parameters. (top): $n=2$, $\omega_x^0=2$, $\omega_y^0=1$, $a=0.024$, $b=0.03$, and polyad number $i=4$. (middle): $n=2$, $\omega_x^0=2$, $\omega_y^0=1$, $a=0.003$, $b=0.01$, and polyad number $i=4$. (bottom): $n=3$, $\omega_x^0=3$, $\omega_y^0=1$, $a=0.017$, $b=0.005$, and polyad number $i=6$. The number of the level counted from the ground state is indicated for each exact quantum level. The approximate resonance Hamiltonian is obtained from the exact polynomial one using Birkhoff–Gustavson perturbation theory (BGPT).

$$\mathscr{I}_1=I,$$

$$\mathscr{I}_2=j_0+\frac{\alpha-\beta}{4\pi\lambda}\left\{j_1\Pi\left(\eta_1;\frac{2\pi\lambda}{\omega^*}\middle|\mu\right)+j_3\Pi\left(\eta_3;\frac{2\pi\lambda}{\omega^*}\middle|\mu\right)+j_4\int_0^{2\pi\lambda/\omega^*}\frac{du}{(1-\eta_1 sn^2(u|\mu))^2}\right\}, \tag{2.9}$$

where $\Pi(\eta_i;u|\mu)$ is the elliptic integral of the third kind

$$\Pi(\eta_i;u|\mu)=\int_0^u\frac{du}{1-\eta_i sn^2(u|\mu)} \tag{2.10}$$

$(\alpha,\beta,\gamma,\delta)$ are the four roots and e the prefactor of the polynomial equation

$$0=n^2K^2J^m(I-J)^n-n^2(\omega I+\epsilon J+\chi_I I^2+\chi_J J^2+\chi_{IJ}IJ-E)^2=e(J-\alpha)(J-\beta)(J-\gamma)(J-\delta) \tag{2.11}$$

for $n=2$: $e=-4\chi_J^2$ and for $n=3$: $e=-9(\chi_J^2+K^2)$.

The four roots are ordered in one of the following ways:

(1) $e>0$, $(\alpha,\beta,\gamma,\delta)\in R^4$, $\gamma\leqslant\delta\leqslant\alpha\leqslant\beta$, $0\leqslant\delta\leqslant\alpha\leqslant I$,

(2) $e<0$, $(\alpha,\beta,\gamma,\delta)\in R^4$, $\delta\leqslant\alpha\leqslant\beta\leqslant\gamma$, $0\leqslant\delta\leqslant\alpha\leqslant I$,

(3) $e<0$, $(\alpha,\beta,\gamma,\delta)\in R^4$, $\beta\leqslant\gamma\leqslant\delta\leqslant\alpha$, $0\leqslant\delta\leqslant\alpha\leqslant I$,

(4) $e<0$, $(\alpha,\delta)\in R^2$, $(\beta,\gamma)\in C^2$, $0\leqslant\delta\leqslant\alpha\leqslant I$. (2.12)

Case (1) was mentioned in Eq. (2.12) to be consistent with Ref. 4. However, it can occur neither for the 1:2 nor for the 1:3 resonance, and therefore needs not be considered in the present paper. The other parameters are expressed as

$$\omega=\omega_2,\quad \epsilon=\frac{m}{n}\omega_1-\omega_2,\quad \chi_I=x_{22},$$

$$\chi_J=\frac{m^2}{n^2}x_{11}-\frac{m}{n}x_{12}+x_{22},\quad \chi_{IJ}=\frac{m}{n}x_{12}-2x_{22},$$

$$K=2\left(\frac{m}{n}\right)^{m/2}k_{mn},$$

$$\eta_1=\frac{\alpha-\delta}{\beta-\delta},\quad \eta_3=\eta_1\frac{I-\beta}{I-\alpha},\quad \mu=\eta_1\frac{\beta-\gamma}{\alpha-\gamma},$$

$$\lambda=\tfrac{1}{2}\sqrt{e(\alpha-\gamma)(\beta-\delta)}=\frac{\omega^*}{2\pi}(2rK(\mu)+2sjK'(\mu))\quad (r,s)\in Z^2,$$

$$j_0=\frac{\beta}{\omega^*}\left[\frac{2-m-n}{2}(\epsilon+\chi_{IJ}I)-\frac{n}{2}\chi_J I+\frac{4-m-n}{2}\chi_J\beta+\frac{m}{2\beta}(E-\omega I-\chi_I I^2)-\frac{n}{2(I-\beta)}(E-(\omega+\epsilon)I-(\chi_I+\chi_J+\chi_{IJ})I^2)\right],$$

$$j_1=(2-m-n)(\epsilon+\chi_{IJ}I)-n\chi_J I+2(4-m-n)\chi_J\beta,$$

$$j_3=-\frac{nI(E-(\omega+\epsilon)I-(\chi_I+\chi_J+\chi_{IJ})I^2)}{(I-\alpha)(I-\beta)},$$

$$j_4=(4-m-n)(\alpha-\beta)\chi_J. \tag{2.13}$$

Semiclassical levels are those values of the energy E, which satisfy

$$\mathscr{I}_1=I=i+\frac{m+n}{2m},$$

$$\mathscr{I}_2=i_2+\tfrac{1}{2},\quad i_2\in Z, \tag{2.14}$$

where i is the polyad number defined in Sec. II B. For a 1:2 and a 1:3 resonance, m is equal to 1 in Eqs. (2.11) to (2.14).

Since this study is restricted to quantum anticrossing levels which belong to the same polyad i, as explained a few lines above, Eq. (2.14) connecting $\mathscr{I}_1=I$ to i demonstrates that it is also restricted to corresponding semiclassical levels which share the same principal quantum number $\mathscr{I}_1$.

It is to be noted, that in Refs. 1 and 2, quantizing trajectories are said to be those trajectories, which satisfy (using the notations of the present paper)

$$\begin{aligned} &\frac{1}{2\pi}\oint_{y=0} I_1\, d\varphi_1 = n_1+\frac{1}{2} \quad n_1\in Z, \\ &\frac{1}{2\pi}\oint_{x=0} I_2\, d\varphi_2 = n_2+\frac{1}{2} \quad n_2\in Z. \end{aligned} \tag{2.15}$$

However, Eq. (2.15) is quite far from the correct EBK quantization rule which has been used to obtain Eq. (2.9)

$$\frac{1}{2\pi}\oint_{C_i} I_1\, d\varphi_1 + I_2\, d\varphi_2 = n_i+\frac{\alpha_i}{4} \quad n_i\in Z. \tag{2.16}$$

In Eq. (2.16), C_i is a closed curve, which is topologically equivalent to one of the minimal circles of the 2D torus supporting the trajectory, and α_i is the associated Maslov index. In Refs. 1 and 2, the quantization conditions in Eq. (2.15) were actually applied to the full polynomial Hamiltonian. In order to check their validity, these conditions can, however, be applied to the approximate resonance Hamiltonian and then compared to Eq. (2.9). Using the coordinates (I,J,θ,ψ) defined in Ref. 4 and the expressions of these coordinates as a function of time, the first phase integral in Eq. (2.15) is found to be equal to $\mathscr{I}_2$. In contrast, for the second phase integral one obtains again $n\mathscr{I}_2$ for class I and II trajectories (that is, trajectories for which the coordinate ψ is a periodic function of time with angular frequency ω^*)[4], $n\mathscr{I}_2-I$ for class III trajectories (where $n\psi$ increases by 2π during a period $2\pi/\omega^*$)[4] and $n\mathscr{I}_2+I$ for class IV trajectories (where $n\psi$ decreases by 2π during a period $2\pi/\omega^*$)[4]. This second phase integral is anyway never equal to the action $\mathscr{I}_1=I$, and its use is particularly to avoid for class I and II trajectories. This is perhaps the reason, why in Ref. 1 the so-called ''trajectory closure method'' seems to have been sometimes used instead of the quantization condition dealing with the second phase integral. No comparative study was attempted concerning this method. Anyway, this unorthodox way of calculating action integrals is perhaps the reason why previous investigations[1–3] were not complete.

III. SEMICLASSICAL BEHAVIOR AT A QUANTUM AVOIDED CROSSING

A. Crossing semiclassical levels

In Refs. 1 and 2, semiclassical levels were reported to cross. An example where such a case occurs is given in Fig. 2. For this 1:2 resonance, it is seen that the quantum avoided crossing between levels ♯7 and ♯8 (counted from the ground state) at $\lambda\approx 0.100$ actually corresponds to crossing semiclassical levels $(\mathscr{I}_1,\mathscr{I}_2)=(11/2,1/2)$ and $(11/2,-5/2)$. However, a much better insight in the semiclassical behavior is gained

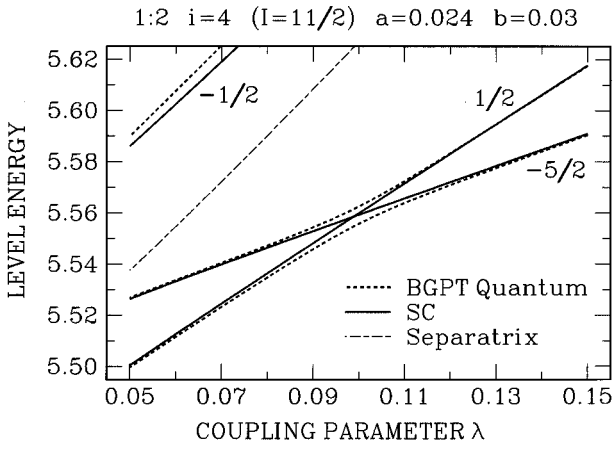

FIG. 2. Plot as a function of λ of the semiclassical and quantum levels for the BGPT resonance Hamiltonian in Eqs. (2.3) and (2.7) for the first set of parameters in Fig. 1: $n=2$, $\omega_x^0=2$, $\omega_y^0=1$, $a=0.024$, $b=0.03$, and polyad number $i=4$, corresponding to $\mathscr{I}_1=I=11/2$. The second semiclassical quantum number $\mathscr{I}_2$ is indicated for each branch of the plot.

when plotting the second action integral $\mathscr{I}_2$ as a function of energy E at a given value of the first action integral $\mathscr{I}_1=I$, that is for a given polyad. Such a plot for $I=11/2$ is given in Fig. 3 for three increasing values of the coupling parameter λ. In these plots, the two levels $\mathscr{I}_2=1/2$ and $\mathscr{I}_2=-5/2$, which anticross quantum mechanically, are represented by filled circles, while the third, mostly noninteracting level $\mathscr{I}_2=-1/2$ is represented by an open circle. It is seen that as λ increases from 0.050 to 0.150, the relative positions of the two levels evolve smoothly: at $\lambda=0.050$, $\mathscr{I}_2=1/2$ lies lower in energy than $\mathscr{I}_2=-5/2$. At $\lambda=0.098$, both levels share the same energy. At $\lambda=0.150$, $\mathscr{I}_2=1/2$ now lies higher in energy than $\mathscr{I}_2=-5/2$. As can be checked from the plot of the $p_2=p_2(q_2)$ Poincaré surfaces of section in Fig. 4, corresponding trajectories vary very little over this range of λ.

Most important in this case is the fact that the two levels lie on separate and superimposed branches of the plot of $\mathscr{I}_2$. Superimposed branches were already evoked in Sec. 4 of Ref. 4. They exist whenever $e<0$ and the four roots of Eq. (2.11) are all real and comprised between 0 and I. The two branches are obtained by ordering the four roots according respectively to cases (2) and (3) in Eq. (2.12). Clearly, the existence of these two branches is needed in order that semiclassical levels can cross in spite of the fact that levels necessarily correspond to half-integral values of $\mathscr{I}_2$.

These results can be interpreted in terms of semiclassical diabatic basis and of quantum dynamical tunneling. Indeed, it is found that avoiding quantum levels can be obtained with excellent accuracy from semiclassical ones by diagonalization of the matrix

$$\begin{pmatrix} E_{1/2}(\lambda) & \frac{\Delta}{2} \\ \frac{\Delta}{2} & E_{-5/2}(\lambda) \end{pmatrix}, \tag{3.1}$$

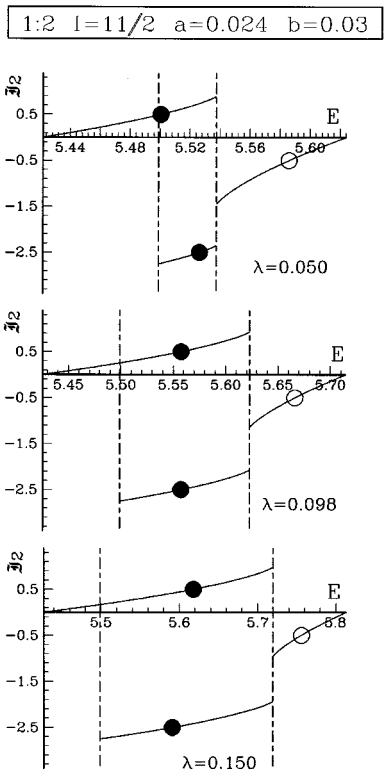

FIG. 3. Plot of the second action integral $\mathscr{I}_2$ as a function of energy E for a given value of the first action integral ($\mathscr{I}_1=I=11/2$) and three increasing values of the parameter λ. Other parameters are the same as in Fig. 2. Filled circles represent those semiclassical levels, whose quantum counterparts anticross, and the open circle the third, mostly noninteracting level.

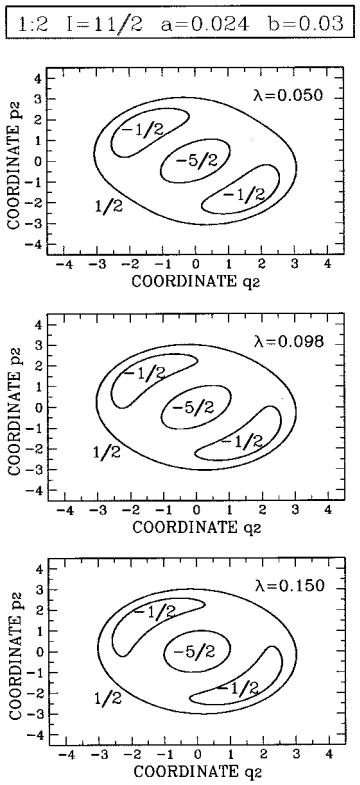

FIG. 4. Poincaré surfaces of section $p_2=p_2(q_2)$ at $q_1=0$ for the quantizing trajectories plotted in Figs. 2 and 3. Parameters are the same as in Figs. 2 and 3. The first semiclassical quantum number $\mathscr{I}_1=I$ is equal to 11/2 for all the trajectories. The second semiclassical quantum number $\mathscr{I}_2$ is indicated for each quantizing trajectory. Resonant trajectories contain two separate islands.

where $E_{1/2}(\lambda)$ and $E_{-5/2}(\lambda)$ stand for the energy of the semiclassical $\mathscr{I}_2=1/2$ and $\mathscr{I}_2=-5/2$ levels. Assuming the numerical value $\Delta=0.0067$ leads to levels which cannot be distinguished from the quantum ones in Fig. 2 for the whole range of λ. Semiclassical levels can therefore be considered as the diabatic basis (crossing levels basis), in terms of which the adiabatic (anticrossing) quantum levels are expressed. At this point, it is worth introducing the concept of quantum dynamical tunneling suggested by Davis and Heller.[11] Quoting Ref. 11, ''tunneling involves an allowed quantum event which fails to take place classically. Dynamical tunneling is the subset of such events which do not involve a classically insurmountable potential barrier.'' This is exactly what is happening here: There exists no energy barrier separating the two classical trajectories (tori) but, nevertheless, a trajectory starting on the $\mathscr{I}_2=1/2$ torus will never end on the $\mathscr{I}_2=-5/2$ torus. In contrast, Eq. (3.1) shows that the quantum system flops forth and back between the two tori and that the frequency of the flops is precisely $\Delta/2$. A further interesting point is that in Ref. 11 quantum dynamical tunneling was demonstrated for those cases, where the symmetry with respect to q_2 is only slightly broken, whereas this symmetry is here completely broken, due to the fact that the three parameters a, b, and λ are all large. Nonetheless, it is seen that tunneling tori can still be found.

B. One trajectory crossing the separatrix

As stated in the previous subsection, the simple description of anticrossing quantum states in terms of dynamical tunneling between semiclassical tori is possible because the two levels lie on separate and superimposed branches of the plot of $\mathscr{I}_2$. In the present and in the next subsections, cases where this condition is not satisfied are going to be studied.

A first example is shown in Figs. 5–7. Compared to the example in Figs. 2–4, only the values of a and b are changed, but this results in the semiclassical system entering the (anti)crossing region with quantum numbers $\mathscr{I}_2=1/2$ and $\mathscr{I}_2=-3/2$, which lie on separate but not superimposed branches of the plot of $\mathscr{I}_2$ (Fig. 6, top). These two branches are separated by a discontinuity, which corresponds to the separatrix, and levels $\mathscr{I}_2=1/2$ and $\mathscr{I}_2=-3/2$ therefore cannot cross. The separatrix is a trajectory reduced to a fixed point in one of Poincaré surfaces of section [the (J,ψ) plane in Ref. 4] with vanishing corresponding frequency $\omega^*=0$, and separates resonant trajectories (i.e., trajectories inside the resonant islands in phase space) from nonresonant trajectories (i.e., trajectories outside the resonant islands). In addition, considering that the semiclassical level spacing might be small at the quantum avoided crossing because classical frequencies are small near the separatrix [see Eq. (25) of Ref. 12, or the work by Cary *et al.*[13]] is not sufficient, since the

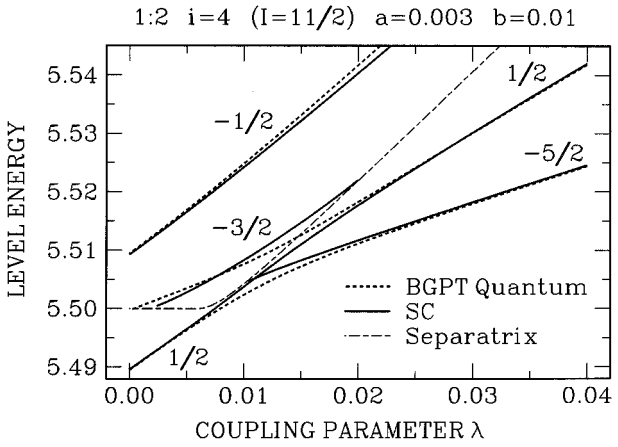

FIG. 5. Plot as a function of λ of the semiclassical and quantum levels for the BGPT resonance Hamiltonian in Eqs. (2.3) and (2.7) for the second set of parameters in Fig. 1: $n=2$, $\omega_x^0=2$, $\omega_y^0=1$, $a=0.003$, $b=0.01$ and polyad number $i=4$, corresponding to $\mathscr{I}_1=I=11/2$. The second semiclassical quantum number $\mathscr{I}_2$ is indicated for each branch of the plot.

energy of semiclassical levels is far from being a simple linear function of ω^*: the energy of the levels varies slowly near the separatrix, whereas the frequency ω^* drops sharply to 0 (see Fig. 2 of Ref. 12).

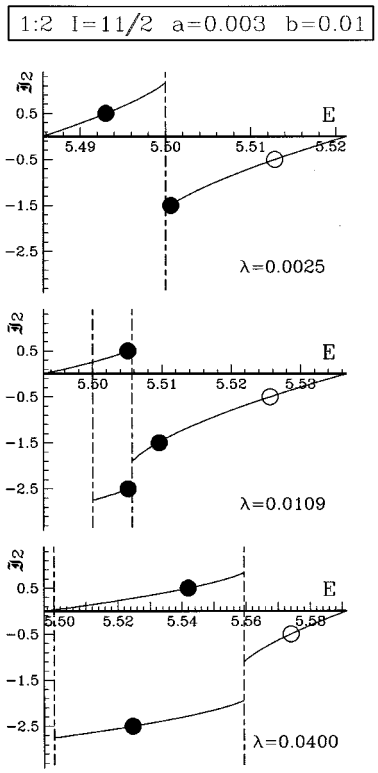

FIG. 6. Plot of the second action integral $\mathscr{I}_2$ as a function of energy E for a given value of the first action integral ($\mathscr{I}_1=I=11/2$) and three increasing values of the parameter λ. Other parameters are the same as in Fig. 5. Filled circles represent those semiclassical levels, whose quantum counterparts anticross, and the empty circle the third, mostly noninteracting level.

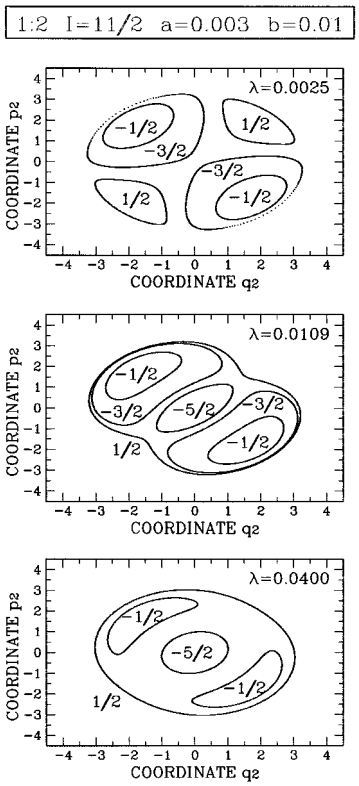

FIG. 7. Poincaré surfaces of section $p_2=p_2(q_2)$ at $q_1=0$ for the quantizing trajectories plotted in Figs. 5 and 6. Parameters are the same as in Figs. 5 and 6. The first semiclassical quantum number $\mathscr{I}_1=I$ is equal to 11/2 for all the trajectories. The second semiclassical quantum number $\mathscr{I}_2$ is indicated for each quantizing trajectory. Resonant trajectories contain two separate islands.

Loosely speaking, the semiclassical system must then find a trick to adapt to the quantum avoided crossing. This trick consists here in one level passing from the inside of the resonance zone, where it satisfies one quantization condition ($\mathscr{I}_2=-3/2$) to the outside, where it satisfies a different quantization condition ($\mathscr{I}_2=-5/2$): As λ is increased, semiclassical levels try to ''follow'' quantum levels and their energy therefore increases, while the gap between the two levels diminishes. Consequently, both levels approach the separatrix as λ increases. When they are too close to the separatrix, somewhat unusual features might arise (Fig. 5 to 7, middle), which will be described below. As the energy of the separatrix does not increase at the same rate as the average energy of both levels (see Fig. 5), one semiclassical level disappears at a given value of λ (here about 0.020), because the branch of $\mathscr{I}_2$ is interrupted by the discontinuity before it reaches the requisite value of $\mathscr{I}_2$ (Fig. 6, bottom). According to the general correspondence, that one quantum level is associated with one semiclassical trajectory, it is expected that another semiclassical level replaces that one which has disappeared. Indeed, it is seen in Figs. 5 and 6 (middle and bottom), that the level with $\mathscr{I}_2=-5/2$ has appeared (it actually appeared at about $\lambda=0.010$). Levels $\mathscr{I}_2=-5/2$ and $\mathscr{I}_2=1/2$ (this latest level simply crosses the quantum avoided crossing) lie on superimposed branches of the plot of $\mathscr{I}_2$ and therefore cross

near the center of the quantum avoided crossing.

So, when going out of the (anti)crossing region, the two quantum levels are associated with two semiclassical levels with respective values of the second quantum number equal to $\mathscr{J}_2=1/2$ and $\mathscr{J}_2=-5/2$, whereas these quantum numbers are equal to $\mathscr{J}_2=1/2$ and $\mathscr{J}_2=-3/2$ before entering it.

Figure 7 shows that, in contrast with the first example in Sec. III A and Fig. 4, the Poincaré surfaces of section—and therefore the trajectories—change drastically from one side of the avoided crossing to the other side, except for the non interacting $\mathscr{J}_2=-1/2$ level which remains mostly unchanged. On the one hand, the resonant $\mathscr{J}_2=-3/2$ trajectory is replaced by the nonresonant $\mathscr{J}_2=-5/2$ trajectory as described above. Both trajectories coexist between $\lambda=0.010$ and $\lambda=0.020$. On the other hand, the trajectory with constant value of $\mathscr{J}_2=1/2$ is also seen to be resonant before the avoided crossing and nonresonant after it. This is explained by the fact that around $\lambda=0.007$ this trajectory crosses what in Refs. 4 and 12 was called the E^- separatrix [see Eq. (A2) in the Appendix for the expression of the energy of the E^- separatrix]. This E^- separatrix is somewhat special: It is a separatrix in the sense that it separates resonant from nonresonant trajectories, but not a ''true'' one, since it does not correspond to any kind of vanishing frequency nor to any discontinuity in the values of the frequencies of the torus or of the action integrals.

Now, let us come back to what happens near the center of the avoided crossing, that is in the region, where at least one semiclassical level is very close to the separatrix. Numerically, one observes that the ''error'' E_Q-E_{SC} between the energy of quantum and semiclassical levels grows significantly when approaching the separatrix (see for instance, the numerical results in Ref. 4). Although this phenomenon has not been thoroughly analyzed, it is probably connected to the fact that trajectories whose energy is close to the separatrix spend most of the time accelerating and decelerating exponentially,[12] which in turn plausibly invalidates the semiclassical approximation. Therefore, near the separatrix problems might occur, which break the usual one-to-one correspondence between quantum and semiclassical levels. In Figs. 5–7 (middle) it is seen, for instance, that two semiclassical levels can be associated with a single quantum level. However, the opposite can also be true, and it happens that some quantum levels remain without any associated semiclassical trajectory for some range of λ (see for instance the plots around $\lambda=0$ in Figs. 5 and 8).

Most important points concerning the example in Figs. 5–7 are therefore (i) the separatrix is absolutely necessary, because semiclassical levels would otherwise be unable both to cross and to anticross; (ii) due to the vicinity of the separatrix, the close correspondence between quantum and semiclassical mechanics is broken near the center of the avoided crossing; (iii) the validity of the description of quantum levels in terms of semiclassical ones is no longer so clear. Keeping with the concept of tunneling between the vectors of the semiclassical diabatic basis, it is seen that the definition of the basis must be adapted as follows: Below, say, $\lambda=0.015$ the basis contains the tori with $\mathscr{J}_2=1/2$ and $\mathscr{J}_2=-3/2$ and above $\lambda=0.015$ the tori with $\mathscr{J}_2=1/2$ and $\mathscr{J}_2=-5/2$. Even with this change, the result is far from being as satisfying as in Sec. III A.

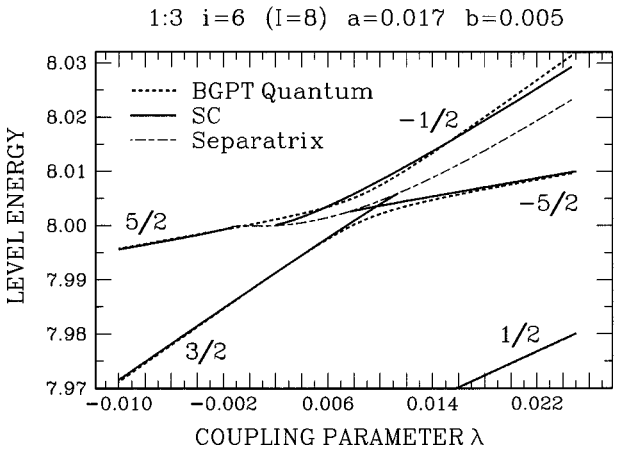

FIG. 8. Plot as a function of λ of the semiclassical and quantum levels for the BGPT resonance Hamiltonian in Eqs. (2.3) and (2.7) for the third set of parameters in Fig. 1: $n=3$, $\omega_x^0=3$, $\omega_y^0=1$, $a=0.017$, $b=0.005$ and polyad number $i=6$, corresponding to $\mathscr{I}_1=I=8$. The second semiclassical quantum number $\mathscr{J}_2$ is indicated for each branch of the plot.

C. Both trajectories crossing the separatrix

A still more complex case is represented in Figs. 8–10, which can nevertheless easily be understood using the discussion in the previous subsection. For this 1:3 resonance, the semiclassical system enters the (anti)crossing region with semiclassical quantum numbers $(\mathscr{J}_1,\mathscr{J}_2)=(8,3/2)$ and $(8,5/2)$. It is seen in Fig. 9 (top) that both levels lie on the same branch of the plot of $\mathscr{J}_2$. Both levels must then cross the separatrix in order to adapt to the quantum avoided crossing: The level $\mathscr{J}_2=5/2$ crosses the separatrix around $\lambda=-0.001$ and is replaced around $\lambda=0.008$ by the level $\mathscr{J}_2=-5/2$. Similarly, the level $\mathscr{J}_2=3/2$ disappears at $\lambda=0.011$ but the level by which it is replaced, $\mathscr{J}_2=-1/2$, already exists for values of λ higher than 0.002. Levels $\mathscr{J}_2=3/2$ and $\mathscr{J}_2=-5/2$ lie on superimposed branches of the plot of $\mathscr{J}_2$ and cross at $\lambda=0.0097$. Therefore, the semiclassical system goes out of the (anti)crossing region with quantum numbers $\mathscr{J}_2=-1/2$ and $\mathscr{J}_2=-5/2$, whereas it entered the region with quantum numbers $\mathscr{J}_2=3/2$ and $\mathscr{J}_2=5/2$. Furthermore, the definition of the semiclassical diabatic basis is here mostly meaningless, since it would require some interpolation between the tori $\mathscr{J}_2=5/2$ and $\mathscr{J}_2=-5/2$ in the range $\lambda=0.001$ to 0.008, where none of these levels exists.

Somewhat surprisingly, it is seen in Fig. 10 that corresponding Poincaré surfaces of section are less complex than for the previous case in Fig. 7. This is mostly due to the fact that the $\mathscr{J}_2=5/2$ trajectory is replaced by the $\mathscr{J}_2=-5/2$ trajectory, which occupies the same region of phase space and is principally characterized by the opposite direction of propagation. The greatest change is due to the other level, which passes from the outside of the resonance region

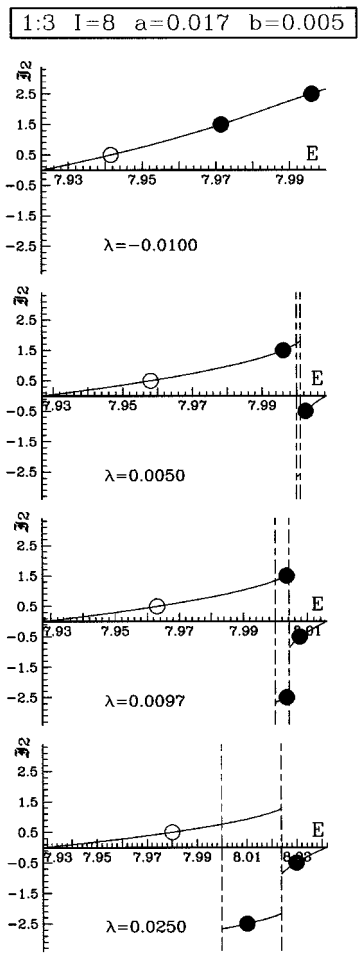

FIG. 9. Plot of the second action integral $\mathscr{I}_2$ as a function of energy E for a given value of the first action integral ($\mathscr{I}_1=I=8$) and four increasing values of the parameter λ. Other parameters are the same as in Fig. 8. Filled circles represent those semiclassical levels, whose quantum counterparts anticross, and the open circle the third, mostly noninteracting level.

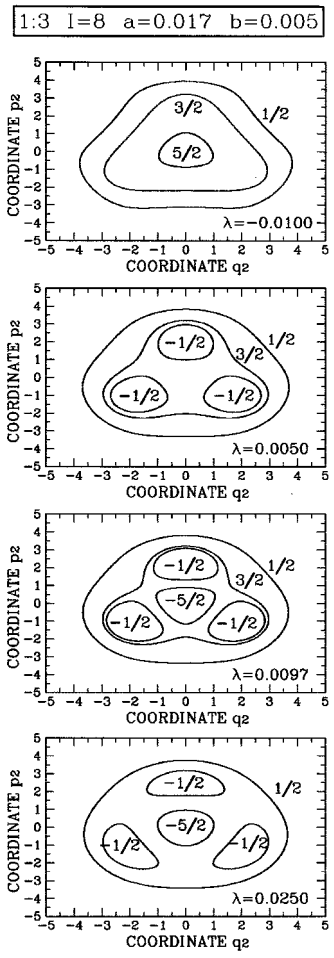

FIG. 10. Poincaré surfaces of section $p_2=p_2(q_2)$ at $q_1=0$ for the quantizing trajectories plotted in Figs. 8 and 9. Parameters are the same as in Figs. 8 and 9. The first semiclassical quantum number $\mathscr{I}_1=I$ is equal to 8 for all the trajectories. The second semiclassical quantum number $\mathscr{I}_2$ is indicated for each quantizing trajectory. Resonant trajectories contain three separate islands.

($\mathscr{I}_2=3/2$) to the inside of the resonance region ($\mathscr{I}_2=-1/2$). As previously, the noninteracting $\mathscr{I}_2=1/2$ level remains mostly unchanged.

APPENDIX: SINGULAR POINTS IN THE PLOT OF $\mathscr{I}_2$

The fact that semiclassical levels cross or do not cross only depends on plots of $\mathscr{I}_2$ like those in Figs. 3, 6, and 9. The expression of $\mathscr{I}_2$ as a function of E and I was derived in Ref. 4 and is reproduced in Eqs. (2.9)–(2.13). However, up to now no method has been given to obtain the first and last point of each branch, and particularly the position of the separatrix. It takes quite a lot of time to obtain these points with good precision when using only Eq. (2.9). In order to enable quicker and more accurate calculations, a simple and precise way to calculate the abscissae of these points is given in this appendix.

The first and last points of each branch in the plot of the action integral $\mathscr{I}_2$ vs the energy E are singular points of the expression of $\mathscr{I}_2$ in Eq. (2.9), except (if $s=0$) for the points on the $\mathscr{I}_2=0$ axis, which are only the limits of the region allowed for E. Singular points can be encountered whenever

$$\begin{aligned}&(1)\ \alpha=\beta \text{ or } \gamma=\delta \text{ (because } \omega^*=0);\\ &(2)\ (\beta=\gamma \text{ or } \alpha=\delta) \text{ and } s\neq 0 \text{ (because } \omega^*=0);\\ &(3)\ I=\alpha \text{ (because } \eta_3 \text{ and } j_3 \text{ are undefined});\\ &(4)\ I=\beta \text{ (because } j_0 \text{ and } j_3 \text{ are undefined}).\end{aligned} \tag{A1}$$

Equation (A1) thus shows that singular points of $\mathscr{I}_2$ correspond either to a double root of Eq. (2.11) or to $J=I$ being a root of this equation [in the cases listed in Eq. (A1), triple roots of Eq. (2.11), like $\alpha=\beta=\gamma$ or $\beta=\gamma=\delta$, were neglected, because they are highly unprobable)]. Let us define E^+ and E^- as in Ref. 4

$$\begin{aligned}E^+&=(\omega+\epsilon)I+(\chi_I+\chi_J+\chi_{IJ})I^2,\\ E^-&=\omega I+\chi_I I^2.\end{aligned} \tag{A2}$$

Examination of Eq. (3.6) of Ref. 4 immediately leads to the conclusion that cases (3) and (4) in Eq. (A1) are satisfied

only if the energy E of the system is equal to E^+. Determination of the energy values at which cases (1) and (2) in Eq. (A1) occur is somewhat more complex. It is achieved by writing that a given value of J is a root of both Eq. (2.11) and of its derivative with respect to J. Two polynomial expressions are obtained, one of degree four and one of degree three with respect to J. Successive linear combinations of these two equations then enable to eliminate J. One is left with a polynomial equation involving only E, I and the parameters defined in Eq. (2.13). This equation is most easily expressed using the reduced coordinates

$$X=\frac{E-E^-}{\chi_J},\quad A=\frac{E^+-E^-}{\chi_J I},\quad B=-\frac{K^2}{e}. \tag{A3}$$

One obtains, for the 1:2 resonance

$$\begin{aligned}0=&(X-AI)^2*[-256X^3+X^2\{-128(A-I)^2+3B(16I-9B+48A)\}+2X\{-8(A-I)^4+3B^2I(3A-2I)+2B(A-I)\\&\times(A^2-22AI-15I^2)\}+BI^2\{-4(A-I)^3+B(A^2-20AI+4BI-8I^2)\}]\end{aligned} \tag{A4}$$

and for the 1:3 resonance

$$\begin{aligned}0=&(X-AI)^3*[256(1-B)X^3+32X^2\{4(A-I)^2+4AB((B+1)I+(B-2)A)+BI^2(B-5)\}+X\{16(A-I)^4\\&+16B(B-2)A^3(A-4I)-24A^2I^2B(B+3)+32ABI^3(B+1)+BI^4(13B-56)\}\\&+BI^3\{4(A-I)^3+4B(I^3-A^3)+3ABI(4A+5I)\}].\end{aligned} \tag{A5}$$

Three remarks are worth doing concerning these equations. First, $X=AI$ (that is $E=E^+$) is solution of both equations. This means that, for $E=E^+$, $J=I$ is a double root of Eq. (2.11). This result was already mentioned in Ref. 12. Second, not all the solutions of Eqs. (A4) and (A5) are actually singular points of $\mathscr{J}_2$. For instance, the solution E might be complex, or correspond to $\gamma=I$, which is not a singular point, or to a double root J which is outside the allowed range $0\leqslant J\leqslant I,\cdots$. Third, points on the $\mathscr{J}_2=0$ axis, which are not singular points in the case $s=0$, but only the limits of the allowed region for E, are nevertheless obtained when solving Eqs. (A4) and (A5), since they correspond to a double root $\alpha=\delta$. Therefore, the first and last points of each branch can all be obtained numerically.

[1] D. W. Noid, M. L. Koszykowski, and R. A. Marcus, J. Chem. Phys. **78**, 4018 (1983).
[2] T. Uzer, D. W. Noid, and R. A. Marcus, J. Chem. Phys. **79**, 4412 (1983).
[3] T. Uzer and R. A. Marcus, J. Chem. Phys. **81**, 5013 (1984).
[4] M. Joyeux, Chem. Phys. **185**, 263 (1994).
[5] G. D. Birkhoff, *Dynamical Systems*, Vol. 9 (AMS Colloquium, New York, 1966).
[6] F. G. Gustavson, Astron. J. **71**, 670 (1966).
[7] R. T. Swimm and J. B. Delos, J. Chem. Phys. **71**, 1706 (1979).
[8] J. P. Pique, M. Joyeux, J. Manners, and G. Sitja, J. Chem. Phys. **95**, 8744 (1991).
[9] P. F. Bernath, M. Dulick, R. W. Field, and J. L. Hardwick, J. Mol. Spectrosc. **86**, 275 (1981).
[10] J. E. Baggott, M. C. Chuang, R. N. Zare, H. R. Dubal, and M. Quack, J. Chem. Phys. **82**, 1186 (1985).
[11] M. J. Davis and E. J. Heller, J. Chem. Phys. **75**, 246 (1981).
[12] M. Joyeux, Chem. Phys. **174**, 157 (1993).
[13] J. R. Cary, P. Rusu, and R. T. Skodje, Phys. Rev. Lett. **58**, 292 (1987).